JACS
JOURNAL OF THE AMERICAN CHEMICAL SOCIETY
Communication
Cite This: J. Am. Chem. Soc. 2018, 140, 13566−13569
pubs.acs.org/JACS

Enabling Homochirality and Hydrothermal Stability in Zn_4O-Based Porous Crystals

Xiang Zhao,[†,‡] Huajun Yang,[†] Edward T. Nguyen,[†] Joshua Padilla,[†] Xitong Chen,[‡] Pingyun Feng,*[,‡] and Xianhui Bu*[,†]

[†]Department of Chemistry and Biochemistry, California State University, Long Beach, California 90840, United States
[‡]Department of Chemistry, University of California, Riverside, Riverside, California 92521, United States

Supporting Information

ABSTRACT: The $[Zn_4O]^{6+}$ cluster is well-known to form the archetypal MOF-5 topology with dicarboxylate ligands. Here we report two new materials (CPM-300 and -301) that show dramatic alteration of topological and chemical behaviors of $[Zn_4O]^{6+}$ clusters. In CPM-300, $[Zn_4O]^{6+}$ untypically forms the MIL-88/MOF-235 type framework with a small pentane-ring-based chiral dicarboxylate. In contrast, in CPM-301, when mediated by $[Zn_9(btz)_{12}]^{6+}$ clusters (btz = benzotriazolate), the MOF-5 topology is regenerated with the same chiral ligand, albeit with alternating $[Zn_4O]^{6+}$ and $[Zn_9(btz)_{12}]^{6+}$ clusters. Importantly, both CPM-300 and CPM-301 are homochiral, hydrothermally stable in boiling water and alcohol, and thermally stable to 440 °C or higher. It is concluded that small methyl groups on the chiral ligand is sufficiently powerful to shield $[Zn_4O]^{6+}$ clusters from degradation by water, even at high temperatures. These results reveal a promising platform for the development of a new class of cluster-based homochiral and hydrothermally stable porous materials.

Over the past two decades, great progress has been made in the development of metal−organic framework (MOF) materials.[1−7] However, a common issue facing most types of MOF materials is their stability, especially toward water which can be present in many applications.[8] For example, the Zn_4O cluster is well liked in MOF chemistry for its outstanding ability to form highly porous frameworks but it is also known for its vulnerability to water damage.[9−11] It is therefore desirble to develop new strategies or mechanisms to address this stability issue.

Constructing MOFs with water-resistant bond types is a straightforward strategy to achieve water tolerability. Examples include zeolitic imidazolate frameworks with Zn−N bonds, as well as MOFs with clusters formed from high-valent metal ions such as Zr^{4+}.[12,13] However, because a large number of MOFs are formed from divalent metal ions (e.g., Cu^{2+}, Zn^{2+}) with carboxylate ligands, a significant impact can be achieved by better controlling factors that affect the stability of these MOFs. Some successful efforts have been made toward this goal, including presynthetic functionalization of ligands with hydrophobic substituents or postsynthetic modifications to introduce hydrophobic moieties.[14,15] Still, few examples are known that can integrate both homochirality and hydrothermal stability.

In this work, we demonstrate a new and versatile platform based on a small chiral ligand, (1*R*,3*R*)-1,2,2-trimethyl-1,3-cyclopentanedicarboxylic acid (also called 1*R*,3*R*-camphoric acid, abbreviated as RR-H_2cam), for constructing cluster-based homochiral and hydrothermally stable MOFs.[16] Two new structures (CPM-300 and CPM-301) containing Zn_4O clusters are reported here. Compared to common dicarboxylate ligands in MOF-5, RR-camphorate offers an enormous stability enhancement in both CPM-300 and CPM-301.

The structures of CPM-300 and CPM-301 were determined by single-crystal X-ray crystallography in chiral $P6_3$ and $R3$ space groups, respectively. CPM-300 comprises uniform Zn_4O clusters with the framework formula of $(Zn_4O)(RR\text{-}cam)_3$. Interestingly, the addition of 1H-benzotriazole leads to the coexistence of two competing types of clusters that are cross-linked into CPM-301 with the formula of $[(Zn_4O)(RR\text{-}cam)_3][Zn_9(btz)_{12}(RR\text{-}cam)_3]$. The successful coassembly between Zn_4 and Zn_9 clusters suggests that the formation of the mixed-cluster MOF-5 type framework is highly tolerant of the size difference between $[(Zn_4O)^{6+}]$ and $[Zn_9(btz)_{12}]^{6+}$ clusters, and is mainly driven by the identical and matching charge (+6, +6) and connectivity (6, 6).

CPM-300 is a rare example of the MIL-88/MOF-235 type structures (the **acs** net) based on the Zn_4O cluster. As shown by MOF-5, the normal behavior of Zn_4O is a 6-connected node with octahedral connectivity, which results in the **pcu**-type structure (Figure 1a). In comparison, the **acs** net is generally formed from trigonal-prismatic building blocks, most commonly M_3O-type trimers as in MIL-88.[17] Thus, it can be said that in CPM-300, Zn_4O tetramer displays a topological behavior much like a M_3O trimer, which is likely caused by the geometry of the chiral ligand. The structure analysis shows that the $Zn_4O(COO)_6$ core still adopts the octahedral geometry as in MOF-5; however, the symmetry reduction from octahedral to trigonal-prismatic occurs when the chiral RR-cam is included (Figure 1b).

Notably, because of the inclusion of enantiopure RR-cam, the entire framework becomes homochiral. CPM-300 features a homochiral hexagonal channel along the *c* axis (Figure 1c). In addition, it is worth noting that the regular trimer-based **acs**

Received: August 9, 2018
Published: October 16, 2018

DOI: 10.1021/jacs.8b08316
J. Am. Chem. Soc. 2018, 140, 13566−13569

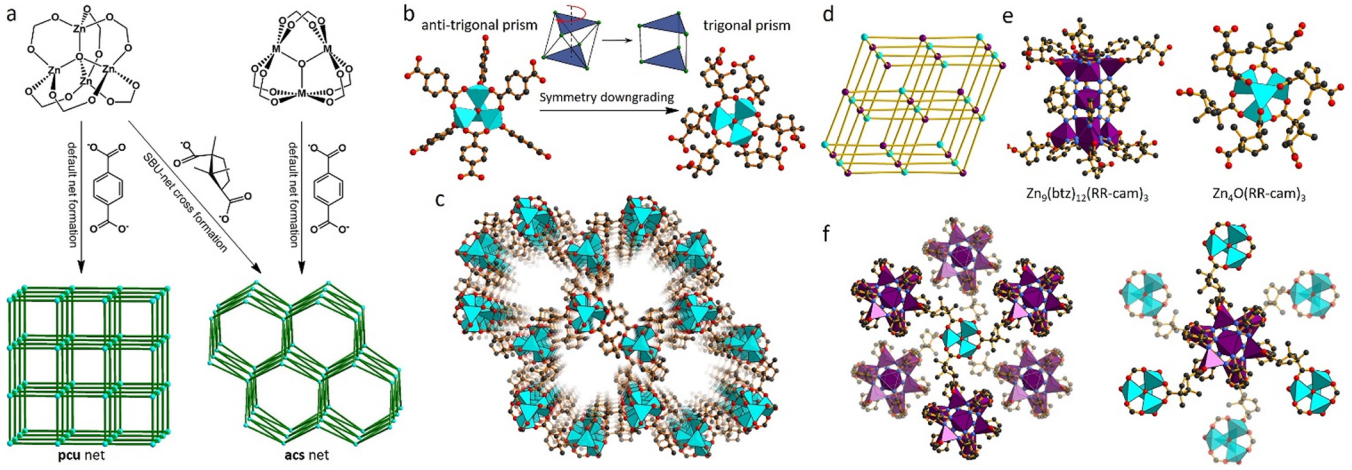

Figure 1. (a) SBU-net cross formation in CPM-300. (b) A comparison of the $Zn_4O(CO_2)_6$ SBU in MOF-5 and CPM-300, showing a symmetry reduction from antitrigonal prism (octahedron) to trigonal prism, when the geometry of ligands are taken into accounts. (c) A perspective view of CPM-300, showing the chiral hexagonal channels along *c* axis. (d) In CPM-301, by introducing the $Zn_9(btz)_{12}$ cluster, the 6-connected Zn_9 and Zn_4 clusters are arranged alternatively to form the **pcu** net again. (e) Illustration of the Zn_9 and Zn_4 clusters in CPM-301. (f) Each Zn_4 cluster is joined to six Zn_9 clusters and vice versa.

net usually has a soft framework. In comparison, the geometry of the **acs** net in CPM-300 is locked by the special geometry of RR-cam and thus CPM-300 has a more rigid framework.

While Zn_4O acts as the only node in CPM-300, it is also possible to connect Zn_4O with other types of SBUs to form 3D frameworks. CPM-301 represents such an example, where in addition to the Zn_4O cluster, a nonameric $[Zn_9(btz)_{12}]^{6+}$ cluster is formed and also serves as a 6-connected node.[18] The two types of 6-connected nodes are bridged by RR-cam to form a **pcu**-type structure (Figure 1d-f). Thus, compared to CPM-300, the incorporation of $[Zn_9(btz)_{12}]^{6+}$ cluster allows the reversal of the framework topology from the chiral-ligand-induced **acs** type back to the **pcu** type.

An important finding of this work is the discovery of extraordinary hydrothermal stability of CPM-300 $Zn_4O(RR\text{-}cam)_3$. Typically, MOFs composed of zinc and carboxylate (e.g., MOF-5) have limited water stability. Surprisingly, in this study, CPM-300, sharing the same Zn_4O unit with MOF-5, was found to exhibit superior water stability. To test the water stability, the crystalline powder sample of CPM-300 was immersed in water at room temperature. The first recheck of its crystallinity was performed after 1 day. To our surprise, the sample maintained high crystallinity. It is noteworthy that common zinc carboxylate MOFs usually lose crystallinity entirely at this point. The sample was further immersed in water for two months and no obvious change in the PXRD pattern was observed (Figure 2a). To further test the stability limit, the CPM-300 sample was refluxed in boiling water, a much harsher condition. It was found that the sample still maintained good crystallinity after refluxing for 2 days. We further found that CPM-300 was also stable in boiling ethanol.

The unusual water stability of CPM-300 prompted us to find the reason behind it. One factor may be the surface property of the sample such as wettability. The wettability test was conducted with packed crystalline powder sample. Figure 3a shows that a stable water droplet can be built up on the surface and will not wet the sample. The contact angle was measured as 138.7°. For comparison, we also performed an experiment with MOF-5 under similar conditions and found that MOF-5 gives an initial contact angle ~17.0° and the water droplet will

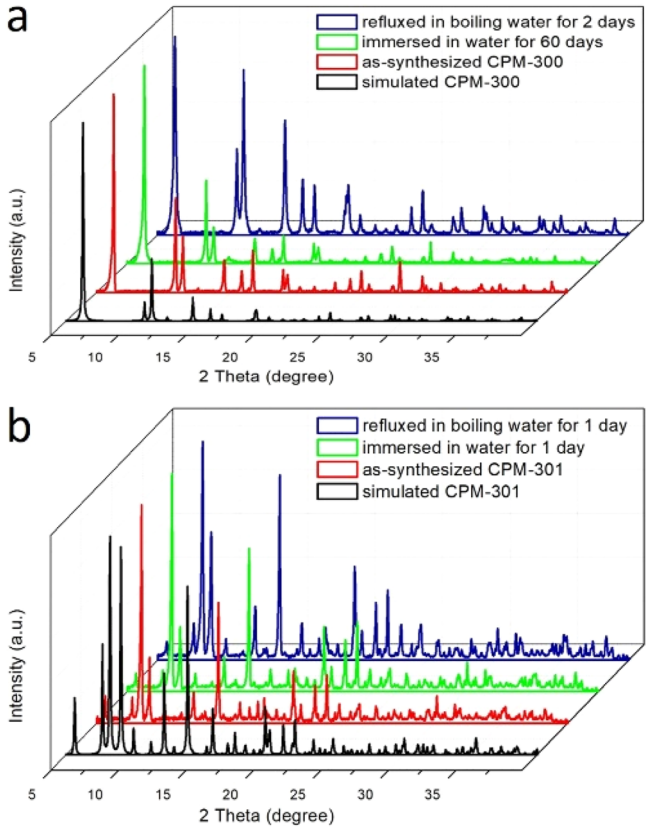

Figure 2. Unusual water stability of CPM-300 and -301 characterized by powder X-ray diffraction (PXRD). The Zn_4O-based CPM-300 can survive in water at room temperature for 60 days or even in boiling water for several days. CPM-301 has similar high stability.

wet the surface immediately upon contact (Figure 3d). Additional wettability test using hexadecane was also performed on CPM-300 (Figure S4). It was observed that the oil droplet will wet the surface immediately upon contact, which again confirm the hydrophobic nature of CPM-300.

To seek the atomic-level understanding of the high water stability of CPM-300, we further compared the crystal

DOI: 10.1021/jacs.8b08316
J. Am. Chem. Soc. 2018, 140, 13566−13569

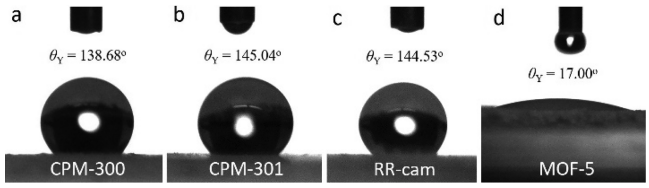

Figure 3. H_2O contact angle measurement on compressed pellet of CPM-300, CPM-301, RR-cam and MOF-5. While stable droplets can be built on the surface of CPM-300 and CPM-301, water droplet will wet the MOF-5 sample immediately upon contact, and complete wetting can be seen in less than 10 s. For RR-cam, with an initial hydrophobic contact angle, the water droplet will gradually wet the sample within 1 min.

structures of MOF-5 and CPM-300. It is found that although both structures share the same building unit (the Zn_4O cluster), the environment around the cluster is totally different (Table S1, Figure 4a). In MOF-5, the Zn_4O cluster is relatively

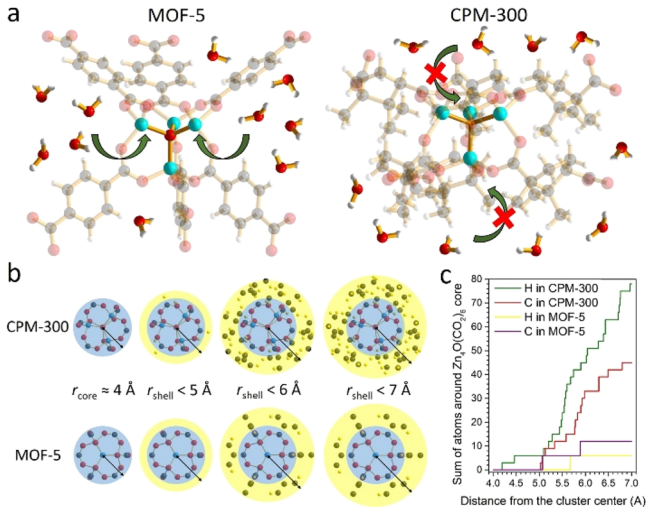

Figure 4. (a) A schematic illustration showing the steric environment around $Zn_4O(CO_2)_6$ clusters in MOF-5 vs in CPM-300. The zinc cluster is accessible by water molecules in MOF-5 while it is protected by hydrophobic groups from RR-cam in CPM-300. (b) A comparison of (001) projection of CPM-300 versus (111) projection of MOF-5 showing the progressive formation of water-resistance shell around the $Zn_4O(CO_2)_6$ core. (c) Incremental count of C and H atoms around the core as a function of distance from the cluster center.

open to the void, which allows water molecule to freely diffuse to the core and attack the zinc cluster. In comparison, the Zn_4O cluster in CPM-300 is surrounded by RR-cam with hydrophobic $-CH_3$ groups to protect it from being attacked by water. A detailed analysis of the coordination environment in two structures shows that within 4 Å from the center μ_4-O is the zinc tetramer cluster core, which needs to be protected (Figure 4b). Within the 0.5 Å shell away from the core, there are already six H atoms from two methyl groups which are closely packed against the cluster, while there are no atoms close to the core in MOF-5 until >5 Å. The difference in the 5−7 Å shell region is also obvious. There are 45 carbons, 72 hydrogens and 3 oxygens in CPM-300 while there are only 18 carbons and 12 hydrogens in the same region in MOF-5. Notably, all 30 atoms in MOF-5 are located in the carboxylate plane, which play less important role as the steric hindrance for water molecules. In contrast, vast majority of the atoms in CPM-300 are out of the carboxylate plane (except 6 carbons) and wraps around the cluster densely. Figure 4c depicts the quantitative plot showing the sum of atoms around the cluster versus the distance to the core. It is believed that the dramatic difference in steric environment around the zinc cluster account for their difference in water resistance.

With the above understanding about the water stability of CPM-300, it is predicted that RR-cam may be capable of enhancing hydrothermal stability of other structure types. A similar structural analysis on CPM-301 shows that there is comparable steric environment around Zn_4O cluster in CPM-301. Indeed, CPM-301 also exhibits an unusual hydrothermal stability. No loss in crystallinity was observed when CPM-301 was immersed in water at room temperature or refluxed in boiling water for 1 day (Figure 2b). Based on the observation of CPM-301 crystals in the boiling water and the subsequent PXRD data, no loss in crystallinity is expected even if CPM-301 is in contact with water for much longer time. We further studied wettability of CPM-301. Stable water droplet can be built on the surface and the contact angle is measured as 145.0°, which suggests the hydrophobic nature of CPM-301 (Figure 3b).

Thermogravimetric analysis shows that CPM-300 and CPM-301 are stable up to 440 and 460 °C, respectively (Figures S7 and S8). Gas sorption measurements were performed on CPM-300. The crystalline samples were treated by refluxing in ethanol for 1 day and were then degassed at 80 °C. CPM-300 shows a BET surface area of 310.5 m^2/g and Langmuir surface area of 429.9 m^2/g, calculated from N_2 sorption at 77K (Figure S9a). It exhibits a uniform and narrow pore size distribution around ~8 Å (Figure S9b), similar to that of zeolite molecular sieve 13X. In addition, it can take up a moderate amount of H_2 (88.4 cm^3/g) at 77 K and ambient pressure (Figure S9d).

In conclusion, a significant progress in the development of crystalline porous materials that combine homochirality with high hydrothermal stability has been made. The synthetic platform is based on a simple, low-cost enantiopure ligand, (1*R*,3*R*)-camphoric acid. We have demonstrated that RR-cam exhibits unique structural features that can generate unexpected framework structures, even from common inorganic building blocks such as Zn_4O clusters. Importantly, RR-cam possesses a molecular structure that seems well suited to protect vulnerable inorganic clusters from water attack, as shown by RR-cam's stabilization effects on both CPM-300 with pure $[Zn_4O]^{6+}$ clusters and CPM-301 with mixed $[Zn_4O]^{6+}$ and $[Zn_9(btz)_{12}]^{6+}$ clusters. We anticipate that RR-cam may serve as a versatile platform for further development of functional materials that combine homochirality, high hydrothermal stability, and uniform porosity.

■ ASSOCIATED CONTENT

Supporting Information

The Supporting Information is available free of charge on the ACS Publications website at DOI: 10.1021/jacs.8b08316.

Experimental section, additional figures on structure descriptions, powder XRD, IR spectra (PDF)

Data for $C_{30}H_{42}O_{13}Zn_4$ (CIF)

■ AUTHOR INFORMATION

Corresponding Authors

*xianhui.bu@csulb.edu

*pingyun.feng@ucr.edu

DOI: 10.1021/jacs.8b08316
J. Am. Chem. Soc. 2018, 140, 13566−13569

ORCID

Xiang Zhao: 0000-0001-7526-8261
Huajun Yang: 0000-0002-4664-4042
Pingyun Feng: 0000-0003-3684-577X
Xianhui Bu: 0000-0002-2994-4051

Notes

The authors declare no competing financial interest.

■ ACKNOWLEDGMENTS

This work was supported by National Science Foundation, Division of Materials Research, under Award #1309347 (X.B.). X.B. thanks the RSCA award from CSULB.

■ REFERENCES

(1) Furukawa, H.; Cordova, K. E.; O'Keeffe, M.; Yaghi, O. M. *Science* **2013**, *341*, 1230444.

(2) (a) Li, B.; Wen, H. M.; Cui, Y.; Zhou, W.; Qian, G.; Chen, B. *Adv. Mater.* **2016**, *28*, 8819. (b) Li, L.; Lin, R.-B.; Krishna, R.; Wang, X.; Li, B.; Wu, H.; Li, J.; Zhou, W.; Chen, B. *J. Am. Chem. Soc.* **2017**, *139*, 7733. (c) Li, P.; He, Y.; Zhao, Y.; Weng, L.; Wang, H.; Krishna, R.; Wu, H.; Zhou, W.; O'Keeffe, M.; Han, Y.; Chen, B. *Angew. Chem., Int. Ed.* **2015**, *54*, 574.

(3) (a) Sava, D. F.; Rohwer, L. E. S.; Rodriguez, M. A.; Nenoff, T. M. *J. Am. Chem. Soc.* **2012**, *134*, 3983. (b) Sava, D. F.; Rodriguez, M. A.; Chapman, K. W.; Chupas, P. J.; Greathouse, J. A.; Crozier, P. S.; Nenoff, T. M. *J. Am. Chem. Soc.* **2011**, *133*, 12398.

(4) (a) Xiao, J.-D.; Han, L.; Luo, J.; Yu, S.-H.; Jiang, H.-L. *Angew. Chem., Int. Ed.* **2018**, *57*, 1103. (b) Jiao, L.; Wang, Y.; Jiang, H.-L.; Xu, Q. *Adv. Mater.* **2018**, *30*, 1703663.

(5) (a) Colinas, I. R.; Silva, R. C.; Oliver, S. R. *Environ. Sci. Technol.* **2016**, *50*, 1949. (b) Oliver, S. R. *Chem. Soc. Rev.* **2009**, *38*, 1868. (c) Fei, H.; Rogow, D. L.; Oliver, S. R. J. *J. Am. Chem. Soc.* **2010**, *132*, 7202.

(6) (a) Peng, Y.; Gong, T.; Zhang, K.; Lin, X.; Liu, Y.; Jiang, J.; Cui, Y. *Nat. Commun.* **2014**, *5*, 4406. (b) Qian, H.-L.; Yang, C.-X.; Yan, X.-P. *Nat. Commun.* **2016**, *7*, 12104. (c) Xiang, S.-C.; Zhang, Z.; Zhao, C.-G.; Hong, K.; Zhao, X.; Ding, D.-R.; Xie, M.-H.; Wu, C.-D.; Das, M. C.; Gill, R.; Thomas, K. M.; Chen, B. *Nat. Commun.* **2011**, *2*, 204. (d) Zhang, S.-Y.; Yang, C.-X.; Shi, W.; Yan, X.-P.; Cheng, P.; Wojtas, L.; Zaworotko, M. *J. Chem.* **2017**, *3*, 281. (e) Ma, L.; Falkowski, J. M.; Abney, C.; Lin, W. *Nat. Chem.* **2010**, *2*, 838.

(7) (a) Lu, H.-S.; Bai, L.; Xiong, W.-W.; Li, P.; Ding, J.; Zhang, G.; Wu, T.; Zhao, Y.; Lee, J.-M.; Yang, Y.; Geng, B.; Zhang, Q. *Inorg. Chem.* **2014**, *53*, 8529. (b) Lin, L.-D.; Li, X.-X.; Qi, Y.-J.; Ma, X.; Zheng, S.-T. *Inorg. Chem.* **2017**, *56*, 4635. (c) Zhao, J.; Wang, Y.; Dong, W.; Wu, Y.; Li, D.; Liu, B.; Zhang, Q. *Chem. Commun.* **2015**, *51*, 9479. (d) Wu, T.; Zhang, J.; Zhou, C.; Wang, L.; Bu, X.; Feng, P. *J. Am. Chem. Soc.* **2009**, *131*, 6111. (e) Zhai, Q.-G.; Bu, X.; Zhao, X.; Li, D.-S.; Feng, P. *Acc. Chem. Res.* **2017**, *50*, 407.

(8) (a) Burtch, N. C.; Jasuja, H.; Walton, K. S. *Chem. Rev.* **2014**, *114*, 10575. (b) Küsgens, P.; Rose, M.; Senkovska, I.; Fröde, H.; Henschel, A.; Siegle, S.; Kaskel, S. *Microporous Mesoporous Mater.* **2009**, *120*, 325.

(9) (a) Li, H.; Eddaoudi, M.; O'Keeffe, M.; Yaghi, O. M. *Nature* **1999**, *402*, 276. (b) Eddaoudi, M.; Kim, J.; Rosi, N.; Vodak, D.; Wachter, J.; O'Keeffe, M.; Yaghi, O. M. *Science* **2002**, *295*, 469. (c) Rosi, N. L.; Eckert, J.; Eddaoudi, M.; Vodak, D. T.; Kim, J.; O'Keeffe, M.; Yaghi, O. M. *Science* **2003**, *300*, 1127. (d) Deng, H.; Doonan, C. J.; Furukawa, H.; Ferreira, R. B.; Towne, J.; Knobler, C. B.; Wang, B.; Yaghi, O. M. *Science* **2010**, *327*, 846. (e) Li, Q.; Zhang, W.; Miljanić, O. Š.; Sue, C.-H.; Zhao, Y.-L.; Liu, L.; Knobler, C. B.; Stoddart, J. F.; Yaghi, O. M. *Science* **2009**, *325*, 855. (f) Koh, K.; Van Oosterhout, J. D.; Roy, S.; Wong-Foy, A. G.; Matzger, A. *J. Chem. Sci.* **2012**, *3*, 2429.

(10) (a) Chae, H. K.; Siberio-Pérez, D. Y.; Kim, J.; Go, Y.; Eddaoudi, M.; Matzger, A. J.; O'Keeffe, M.; Yaghi, O. M. *Nature* **2004**, *427*, 523. (b) Koh, K.; Wong-Foy, A. G.; Matzger, A. J. *J. Am. Chem. Soc.* **2009**, *131*, 4184. (c) Koh, K.; Wong-Foy, A. G.; Matzger, A. J. *J. Am. Chem. Soc.* **2010**, *132*, 15005. (d) Furukawa, H.; Ko, N.; Go, Y. B.; Aratani, N.; Choi, S. B.; Choi, E.; Yazaydin, A. Ö.; Snurr, R. Q.; O'Keeffe, M.; Kim, J.; Yaghi, O. M. *Science* **2010**, *329*, 424. (e) Zhang, Y.-B.; Furukawa, H.; Ko, N.; Nie, W.; Park, H. J.; Okajima, S.; Cordova, K. E.; Deng, H.; Kim, J.; Yaghi, O. M. *J. Am. Chem. Soc.* **2015**, *137*, 2641. (f) Zhang, M.; Feng, G.; Song, Z.; Zhou, Y.-P.; Chao, H.-Y.; Yuan, D.; Tan, T. T. Y.; Guo, Z.; Hu, Z.; Tang, B. Z.; Liu, B.; Zhao, D. *J. Am. Chem. Soc.* **2014**, *136*, 7241. (g) Gedrich, K.; Senkovska, I.; Baburin, I. A.; Mueller, U.; Trapp, O.; Kaskel, S. *Inorg. Chem.* **2010**, *49*, 4440. (h) Liu, L.-L.; Yu, C.-X.; Sun, J.; Meng, P.-P.; Ma, F.-J.; Du, J.-M.; Ma, L.-F. *Dalton Trans* **2014**, *43*, 2915.

(11) (a) Greathouse, J. A.; Allendorf, M. D. *J. Am. Chem. Soc.* **2006**, *128*, 10678. (b) Kaye, S. S.; Dailly, A.; Yaghi, O. M.; Long, J. R. *J. Am. Chem. Soc.* **2007**, *129*, 14176. (c) Guo, P.; Dutta, D.; Wong-Foy, A. G.; Gidley, D. W.; Matzger, A. J. *J. Am. Chem. Soc.* **2015**, *137*, 2651. (d) Ming, Y.; Purewal, J.; Yang, J.; Xu, C.; Soltis, R.; Warner, J.; Veenstra, M.; Gaab, M.; Müller, U.; Siegel, D. J. *Langmuir* **2015**, *31*, 4988.

(12) (a) Park, K. S.; Ni, Z.; Côté, A. P.; Choi, J. Y.; Huang, R.; Uribe-Romo, F. J.; Chae, H. K.; O'Keeffe, M.; Yaghi, O. M. *Proc. Natl. Acad. Sci. U. S. A.* **2006**, *103*, 10186.

(13) (a) Cavka, J. H.; Jakobsen, S.; Olsbye, U.; Guillou, N.; Lamberti, C.; Bordiga, S.; Lillerud, K. P. *J. Am. Chem. Soc.* **2008**, *130*, 13850. (b) Furukawa, H.; Gándara, F.; Zhang, Y. B.; Jiang, J.; Queen, W. L.; Hudson, M. R.; Yaghi, O. M. *J. Am. Chem. Soc.* **2014**, *136*, 4369. (c) Wang, B.; Lv, X.-L.; Feng, D.; Xie, L.-H.; Zhang, J.; Li, M.; Xie, Y.; Li, J.-R.; Zhou, H.-C. *J. Am. Chem. Soc.* **2016**, *138*, 6204. (d) Zhang, W.; Hu, Y.; Ge, J.; Jiang, H.-L.; Yu, S.-H. *J. Am. Chem. Soc.* **2014**, *136*, 16978. (e) DeCoste, J. B.; Peterson, G. W.; Jasuja, H.; Glover, T. G.; Huang, Y.-g.; Walton, K. S. *J. Mater. Chem. A* **2013**, *1*, 5642.

(14) (a) Nguyen, J. G.; Cohen, S. M. *J. Am. Chem. Soc.* **2010**, *132*, 4560. (b) Yang, J.; Grzech, A.; Mulder, F. M.; Dingemans, T. *Chem. Commun.* **2011**, *47*, 5244. (c) Sun, Q.; He, H.; Gao, W.-Y.; Aguila, B.; Wojtas, L.; Dai, Z.; Li, J.; Chen, Y.-S.; Xiao, F.-S.; Ma, S. *Nat. Commun.* **2016**, *7*, 13300. (d) Deria, P.; Mondloch, J. E.; Tylianakis, E.; Ghosh, P.; Bury, W.; Snurr, R. Q.; Hupp, J. T.; Farha, O. K. *J. Am. Chem. Soc.* **2013**, *135*, 16801. (e) Cai, Q.; Zhang, Y.; Huang, Y.; Marder, S. R.; Walton, K. S. *Cryst. Growth Des.* **2012**, *12*, 3709.

(15) (a) Zhang, Z.; Nguyen, H. T. H.; Miller, S. A.; Ploskonka, A. M.; DeCoste, J. B.; Cohen, S. M. *J. Am. Chem. Soc.* **2016**, *138*, 920. (b) Ding, N.; Li, H.; Feng, X.; Wang, Q.; Wang, S.; Ma, L.; Zhou, J.; Wang, B. *J. Am. Chem. Soc.* **2016**, *138*, 10100. (c) Gamage, N.-D. H.; McDonald, K. A.; Matzger, A. J. *Angew. Chem., Int. Ed.* **2016**, *55*, 12099.

(16) Zhao, X.; Nguyen, E. T.; Hong, A. N.; Feng, P.; Bu, X. *Angew. Chem., Int. Ed.* **2018**, *57*, 7101.

(17) (a) Sudik, A. C.; Côté, A. P.; Yaghi, O. M. *Inorg. Chem.* **2005**, *44*, 2998. (b) Serre, C.; Millange, F.; Surble, S.; Férey, G. *Angew. Chem., Int. Ed.* **2004**, *43*, 6285.

(18) (a) Li, Y.-W.; He, K.-H.; Bu, X.-H. *J. Mater. Chem. A* **2013**, *1*, 4186. (b) Biswas, S.; Tonigold, M.; Speldrich, M.; Kögerler, P.; Volkmer, D. *Eur. J. Inorg. Chem.* **2009**, *2009*, 3094.

DOI: 10.1021/jacs.8b08316
J. Am. Chem. Soc. 2018, 140, 13566−13569